UC Davis

UC Davis Previously Published Works

Title

Can a commercially available EPID dosimetry system detect small daily patient setup errors for cranial IMRT/SRS?

Permalink

https://escholarship.org/uc/item/6wc3h61j

Journal

Practical Radiation Oncology, 7(4)

ISSN

1879-8500

Authors

Hsieh, Emmelyn S
Hansen, Katherine S
Kent, Michael S
et al.

Publication Date

2017-07-01

DOI

10.1016/j.prro.2016.12.005

Peer reviewed

eScholarship.org Powered by the California Digital Library
University of California

Practical Radiation Oncology (2017) 7, e283–e290

practical radiation oncology
pro
www.practicalradonc.org

Basic Original Report

Can a commercially available EPID dosimetry system detect small daily patient setup errors for cranial IMRT/SRS?

Emmelyn S. Hsieh BS [a], Katherine S. Hansen DVM [b], Michael S. Kent DVM [b], Sanjeev Saini BS [c], Sonja Dieterich PhD [d,*]

[a]*School of Veterinary Medicine, University of California, Davis, Davis, California*
[b]*Department of Surgical and Radiological Sciences, UC, Davis School of Veterinary Medicine, Davis, California*
[c]*Sun Nuclear Inc, Melbourne, Florida*
[d]*Department of Radiation Oncology, University of California Davis School of Medicine, Sacramento, California*

Received 28 June 2016; revised 26 November 2016; accepted 20 December 2016

Abstract

Purpose: The purpose of this study was to determine if the Sun Nuclear PerFRACTION electronic portal imager device dosimetry software would be able to detect setup errors in a clinical setting and would be able to correctly identify the direction in which the setup error was introduced.

Methods and materials: A 7-field intensity modulated radiation therapy (IMRT) treatment plan for a centrally located tumor was developed for 1 phantom and 5 canine cadaver heads. Systematic setup errors were introduced by manually moving the treatment couch by 1, 3, and 5 mm in each translational direction to assess stereotactic radiation surgery (SRS), IMRT, and 3-dimensional (3D) treatment tolerances after the initial alignment was performed. An angular setup error of 5° yaw was also assessed. The delivered treatment fluence was automatically imported in the PerFRACTION software and compared with the baseline fluence.

Results: In the canine phantom, a 5-mm shift was undetected by gamma analysis, and up to a 2-cm shift had to be introduced for the gamma pass rate of 3%/3 mm to fall below a 95% pass rate criterion. The same 5-mm shift using 3% difference caused the pass rates for 2 fields to drop below the 95% tolerance. For each respective translational shift, the affected beam angles were consistent across the cadaver heads and correlated with the direction of translational shift. The best field pass rate, worst field pass rate, and average pass rate across all 7 fields was analyzed to develop clinical guidance on parameter settings for SRS, IMRT, and 3D tolerances.

Conclusions: PerFRACTION 2-dimensional mode successfully detected setup errors outside the systematic error tolerance for SRS, IMRT, and 3D when an appropriate analysis metric and pass/fail criteria was implemented. Our data confirm that percent difference may be more sensitive in detecting plan failure than gamma analysis.

© 2017 American Society for Radiation Oncology. Published by Elsevier Inc. All rights reserved.

Conflicts of interest: S.D. has a research agreement with Sun Nuclear, Inc., and is an editor of *Practical Radiation Oncology*. S.S. is an employee of Sun Nuclear, Inc. E.H., K.H., and M.K.: None.

* Corresponding author. Department of Radiation Oncology, University of California Davis School of Medicine, 4105 X Street, Sacramento, CA 95817.
E-mail address: sdieterich@ucdavis.edu (S. Dieterich).

http://dx.doi.org/10.1016/j.prro.2016.12.005
1879-8500/© 2017 American Society for Radiation Oncology. Published by Elsevier Inc. All rights reserved.

Introduction

In the late 1990s, methods to use an electronic portal imager device (EPID) were developed to measure the exit fluence during radiation therapy treatment fractions as a tool for dose delivery quality assurance.[1,2] EPID dosimetry technology was soon implemented as part of clinical research at the Netherlands Cancer Institute to monitor treatment delivery for a large number of patients. An early publication by Mans et al[3] and the update by Mijnheer et al[4] report on the numbers of patients monitored, error rates, and error causes found in these studies. Clinical tolerance level settings using gamma (Low et al[5]) were designed to yield what was considered an acceptable error rate (i.e., fulfilling the goal to flag major treatment deviations without exceeding the staff time available to review and analyze flagged treatments).

An increased focus on error rates and error reporting since the publication of the 2009 *New York Times* article series on errors in radiation oncology by Bogdanich[6] has led to studies on the effectiveness of error prevention techniques used in the clinical setting. Ford et al[7] demonstrated that EPID dosimetry ranks highly in effectiveness to detect errors among the available tools for error prevention. In a follow-up paper by Bojechko et al,[8] EPID in vivo dosimetry was analyzed with respect to its capability to detect errors or near misses ranking high on the severity scale from an in-house error reporting system. First-day and during-treatment EPID dosimetry were shown to be highly effective in detecting errors.

Published data on clinical EPID dosimetry implementations to date have focused on detecting major errors. With the Food and Drug Administration approval of commercial EPID dosimetry software solutions, the technology has become more widely available for clinical implementation because it requires less staff time to develop, commission, and maintain the software. These resources can now be put toward efforts to explore new clinical applications of EPID dosimetry such as monitoring systematic patient setup errors of 5 mm or less.

The PerFRACTION software (Sun Nuclear Corporation, Melbourne, FL) is one example of a new vendor product that is used to capture transmitted radiation fluence data using the EPID for delivered versus planned dose comparison. An earlier study by Nelms et al[9] evaluated the accurate image to dose plane conversion over a variety of conditions. At the time of this study, the PerFRACTION software was under clinical evaluation; a study assessing the accuracy and sensitivity of the software had not yet been published. We hypothesized that the PerFRACTION software would be able to detect setup errors outside the tolerance for intensity modulated radiation therapy (IMRT) and stereotactic radiation surgery (SRS) in a clinical setting and would be able to correctly identify the direction in which the setup error was introduced. Additionally, we hypothesized that our study could provide more insight into which quality assurance (QA) analysis tools and specific pass/fail criteria would be most appropriate for detecting the types of clinical errors evaluated in this study. To test the PerFRACTION software in a more realistic clinical environment than a rigid phantom can provide, we used a range of dog cadaver heads closely matched to the typical cranium size found in pediatric and adult human patients. As a result, this study is more clinically relevant for veterinary patients and is translatable to human radiation oncology as well.

Methods and materials

Patients

The experiments were conducted using the Varian TrueBeam linear accelerator (Varian Medical Systems, Palo Alto, CA) at the Center for Companion Animal Health. A phantom made of Virtual Water (Standard Imaging, Middleton, WI) with an embedded canine skull and molded from a canine head was used to gather preliminary data and refine the experimental technique before using the cadaver heads (Fig 1).

After the experimental technique was established, 5 canine cadaver heads were collected from the Anatomic Pathology Service. The cadavers were donated to the school for unrestricted use after the dogs had died. Of the 5 heads, 2 were of medium-sized breeds and 3 were of large-sized breeds. One head was from a mastiff mixed breed with brachy- to mesocephalic features; the other 4 were from dolichocephalic mixed breeds. The separations for the heads were 11.0, 12.2, 14.1, 15.9, and 18.2 cm. The heads were stored frozen until used. We assumed that the heads being frozen would not affect the results of our measurement.

Procedures

Each cadaver head remained frozen throughout the entire testing procedure. A custom head mask and deformable pillow was created for each head to match the immobilization used in clinical practice.[10] A simulation computed tomography scan (Lightspeed 16, General Electric, Milwaukee, WI) of the head was obtained from the diagnostic imaging and was imported into Eclipse (Version 11) treatment planning software system. Images were acquired with 1.25-mm collimation in axial mode. Acquisition parameters were 120 kV and 150 mA, with the exception of 1 larger head labeled RT 4 that used 120 kV and 200 mA. These parameters are comparable to parameters used for computed tomography simulation of cranial patients at the University of California Davis Medical Center (120 kV, 140 mA).

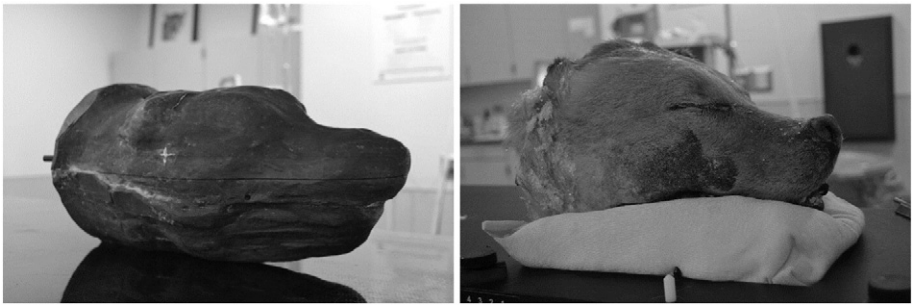

Figure 1 Lateral views of the Virtual Water phantom head and 1 of the cadaver heads.

A 7-field IMRT plan using 200 cGy fractions was created for a simulated intranasal tumor (Fig 2). The size and location of the target was chosen such that none of the beams had flash, mimicking a cranial SRS or IMRT treatment. The body, bones, brain, eyes, and optic apparatus were contoured as organs at risk for radiation exposure. The entire nasal cavity, including the maxillary and frontal sinuses, was contoured to mimic canine intranasal tumors commonly treated with radiation therapy. Plans were optimized to deliver 95% of the prescribed dose to the entire planning target volume (PTV) while minimizing the dose to the contoured normal organs at risk.

A QA plan was created and exported to the linear accelerator for delivery quality assurance (DQA) testing using a 2-dimensional (2D) detector array device (MapCHECK, Sun Nuclear Corporation). In addition, the treatment plan was exported to the PerFRACTION software, treated in air ("fraction 0") and compared with the MapCHECK result. This served as a secondary check that the plan was deliverable as planned from the technical perspective.

Once the baseline measurements were acquired, the cadaver head was then set up and aligned using cone beam computed tomography image guidance. The cadaver head was treated, and the EPID images were captured and used as the baseline measurement for the rest of the trial runs. Systematic setup errors were simulated by shifting each cadaver head by 1, 3, and 5 mm in each translational direction (cranial, ventral, lateral). An angular setup error of 5° yaw was also assessed. The treatments were repeated 3 times, and EPID data were captured for each setup error shift. In summary, 3 distances repeated in triplicate for 3 spatial directions resulted in 27 treatments. The baseline and angle each repeated in triplicate added another 6 treatments. The overall time required to complete all 33 treatments per cadaver was about 5.5 hours with about 7 to 10 minutes per treatment.

The EPID images and trajectory log files were automatically imported by the PerFRACTION software for each treatment. Of the 2D data analysis options PerFRACTION offered at the time of this study (gamma, distance to agreement [DTA], percent difference), we evaluated both gamma and percent difference. Analysis criteria of 3%/3 mm and 3%/1 mm were used for gamma. For the percent difference, we used 3% and 1% as criteria. The software then calculated a pass rate for each IMRT field (Fig 3). The software also automatically calculated if there was a translational shift of the measured data that could increase the pass rate.

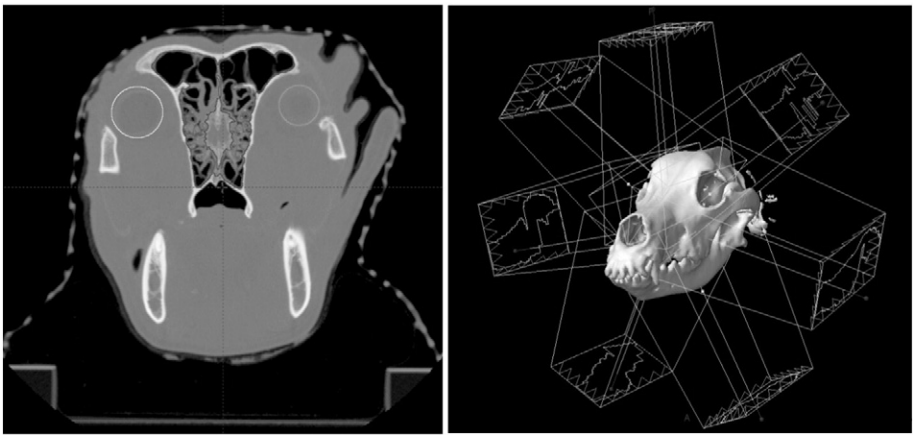

Figure 2 Example of contouring and intensity modulated radiation therapy planning for cadaver head RT 1.

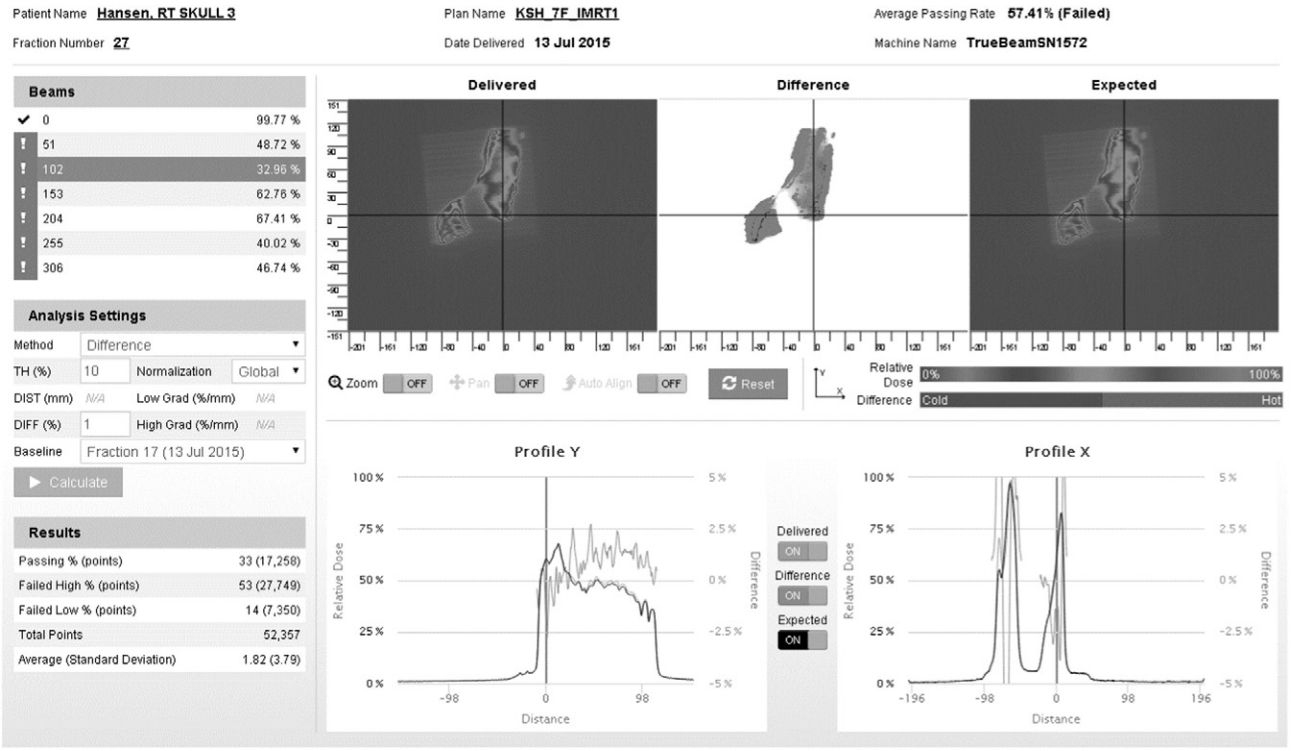

Figure 3 Example of a fraction in PerFRACTION analysis for cadaver dog number 3 treated with an intensity modulated radiation therapy treatment plan and a 5-mm ventral shift. The left column shows the numerical analysis for each individual field and analysis settings. The top row shows, from left to right, the delivered fluence; difference between expected and delivered fluence; and expected fluence for the 102° beam angle highlighted in the upper left. The bottom row shows the cross-sectional profiles at positions indicated by the black lines in the top row.

Data analysis

Microsoft Excel was used to organize the collected data. Statistical analysis was done using GraphPad Prism 6 (GraphPad Software, Inc., La Jolla, CA). Means and standard deviations were calculated. To compare dose pass rates for each shift and beam angle, a 2-way repeated measures analysis of variance was done with a Tukey test to adjust for multiple comparisons and look for differences between groups.

Results

Gamma analysis for Virtual Water phantom head

The baseline gamma results yielded a 100% pass rate for both canine phantom and all 5 cadaver heads. Of the several QA analysis tools available to evaluate a treatment plan, we chose the most commonly used: gamma and percent difference. Gamma proved to be less sensitive to setup shifts than percent difference (Table 1). In the canine phantom, a 5-mm left shift was undetected by gamma analysis, and up to a 2-cm shift had to be introduced for the average gamma pass rate of 3%/3 mm to fall below a 95% pass rate criteria. A 1-cm shift was needed to cause the gamma pass rate for the field perpendicular to the couch shift to fall below 95%. In contrast, the same shift using 3% difference caused the pass rates for 2 fields to drop below the 95% tolerance. Because gamma proved insensitive to the small shifts to be studied in this work, the subsequent analysis was focused on the more sensitive DTA metric.

Percent difference for translational shifts and yaw

For each respective translational shift, the affected beam angles were consistent across the cadaver heads and correlated with the direction of translational shift (Fig 4). For instance, a ventral shift affected beam angles 255° and 102°, whereas a left shift affected beam angles 204°, 0°, and 153°. Values were statistically significant between the 1-, 3-, and 5-mm shifts in all directions for all beam angles except for 0° with ventral shifts ($P < .0001$).

In the different cadaver heads, the gamma pass rate per beam angle and shift varied and correlated with changes in source-to-surface distance and separation (Fig 5).

Table 1 Comparison of gamma analysis and percent difference quality assurance analysis tools on the canine phantom head

Gamma analysis (3.0001%/1.0001 mm)	204°	255°	306°	0°	51°	102°	153°	Average
5-mm left shift 1	98.53	99.99	100	99.44	99.38	100	97.69	99.29
5-mm left shift 2	98.29	99.99	100	99.45	99.42	100	97.77	99.27
5-mm left shift 3	98.38	100	100	99.42	99.42	100	97.72	99.28
Average	98.4	99.99	100	99.44	99.41	100	97.73	99.28
1-cm left shift	97.25	99.25	99.04	97.54	96.8	99.99	**90.47**	97.19
2-cm left shift	97.35	98.04	**90.57**	**85.89**	**93.18**	99.71	**66.58**	**90.19**
Percent difference (3.0001%)								
5-mm left shift 1	**94.49**	99.89	99.33	97.36	98.42	99.98	**90.80**	97.18
5-mm left shift 2	**94.04**	99.88	99.38	97.45	98.48	99.89	**91.10**	97.17
5-mm left shift 3	**94.18**	99.89	99.35	97.43	98.52	99.91	**90.98**	97.18
Average	**94.24**	99.89	99.35	97.41	98.47	99.93	**90.96**	97.18

Measurements that did not have a 95% or higher pass rate are in bold.

Table 2 summarizes the analysis results for all translational and rotational shifts for the canine phantom and 5 cadaver heads. The best field pass rate, worst field pass rate, and average pass rate across all 7 fields are listed.

Discussion

Excluding any major delivery issues, the goal of implementing in vivo EPID dosimetry is to detect systematic positioning errors that may exceed the PTV and planning organ-at-risk volume margins. In a recent paper by Bojecko et al,[11] the authors state that patient position displacements of 5 and 10 mm in each of the 3 cardinal directions in their selected patient cohort was not readily detectable using the gamma index. Our results confirmed the findings of Kruse,[12] who determined that per-field gamma analysis was a poor predictor of dosimetric accuracy. Although Kruse focused on the ability of DQA to detect plans that were undeliverable because of modulation factors exceeding the machine's delivery capabilities, he found that the DTA component of gamma was masking errors in the gradient-rich fluence map of individual IMRT fields. Our study contained plans with similar modulation factors to clinical plans; nevertheless, we found that the DTA component of gamma masked the setup errors we introduced as well. Because the changes in the fluence introduced by our shifts were small given the small changes in source-to-surface distance and separation, and the lack of flash for these centrally located nasal tumors, our gamma pass rates were considerably higher for unacceptable shifts than for the unacceptable IMRT plans measured by Kruse.

When we removed the masking effect of the DTA by using percent difference for data analysis, per-field 2D EPID dosimetry was indeed capable of flagging the fields for which the dosimetric changes introduced by the shifts were largest. Based on our data, we then developed pass rate criteria that would be able to detect shifts exceeding specific tolerances (Table 3). For 3 of the 7 tolerance levels, the canine phantom was the skull shape requiring the strictest settings. One possible cause for this could be the absence of air cavities in the canine phantom, because a shift in air cavity location would change the transmission dose to a much larger extent than a shift in bony anatomy alone. Given our small sample size, we cannot state the specificity and sensitivity of these thresholds with respect to anatomic features or other factors. In the clinical setting, the question then becomes if the tolerance levels should be set to the most or least stringent. If the clinical goal is to detect the major outliers only, selecting the least stringent tolerance level would be a reasonable choice. If, on the other hand, the goal of EPID data acquisition is to reduce the daily setup uncertainty, the more stringent tolerance settings should be used. For delivered fractions exceeding the tolerance, physicists can then evaluate which beam angles passed or failed and thereby deduce in which direction the setup error was most likely introduced. This information will in turn enable the treatment team to focus their root cause analysis to identify the cause for the dose delivery variation. One should note that the investment of physics/therapy time and the number of false positives increase as the tolerance levels are tightened.

A possible risk with institutions developing their own pass/fail criteria was pointed out by Kry et al, stating: "When IROC Houston interpreted whether a plan had failed the institution's IMRT QA, many more plans were described as failing."[13] This finding is a strong indication that standardized pass-fail criteria could be useful in standardizing quality of care across clinics. Nelms et al concur: "Many forms of relevant systematic errors can go undetected when the currently prevalent metrics for IMRT/[volumetric arc therapy] commissioning are used. If alternative methods and metrics are used instead of (or in addition to) the conventional metrics, these errors

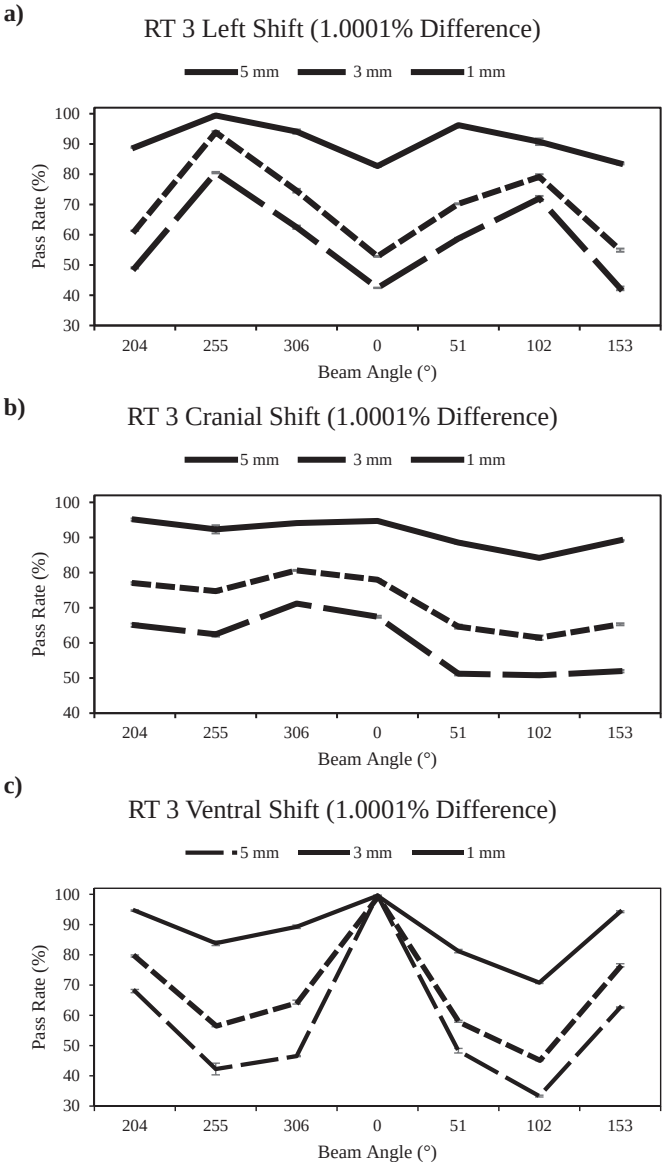

Figure 4 Variations in beam angle pass rate with three translational shifts in (a) left, (b) cranial, and (c) ventral directions for cadaver head RT 3.

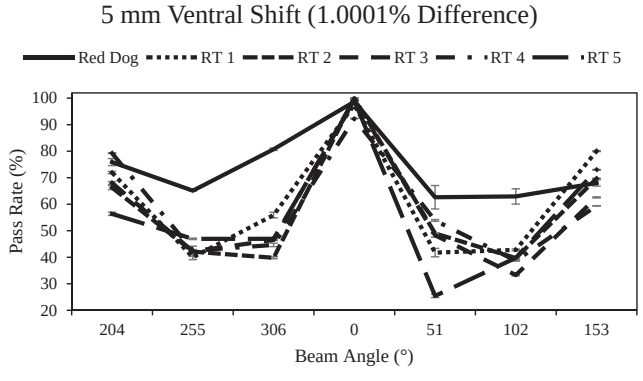

Figure 5 Variations in severity of plan failure depending on shape of the cadaver head.

Table 2 Summary of findings for translational and yaw shifts in the Red Dog phantom and all cadaver heads. (A) data for 3% difference. (B) data for 1% difference

Patient	Pass rate criteria	5 mm left	5 mm cranial	5 mm ventral	3 mm left	3 mm cranial	3 mm ventral	1 mm left	1 mm cranial	1 mm ventral	Yaw
3% difference											
Canine Phantom	Best field pass rate	99.93	99.04	100.00	100.00	99.71	100.00	100.00	100.00	100.00	99.69
	Worst field pass rate	90.96	94.63	95.34	94.58	97.46	97.52	98.14	99.14	99.14	94.66
	Average field pass rate	97.18	97.37	97.08	98.10	98.70	98.78	99.65	99.85	99.73	97.87
RT 1	Best field pass rate	97.99	97.03	99.97	99.44	98.60	99.94	100.00	99.83	100.00	98.16
	Worst field pass rate	87.54	92.71	76.56	92.51	96.38	86.64	98.76	98.92	96.53	89.42
	Average field pass rate	93.07	94.70	87.79	96.19	97.27	93.62	99.54	99.48	98.59	95.37
RT 2	Best field pass rate	99.73	95.71	100.00	99.94	98.10	100.00	100.00	99.97	100.00	99.70
	Worst field pass rate	79.95	84.28	74.46	91.20	92.68	84.39	98.85	99.40	98.58	90.55
	Average field pass rate	91.39	92.36	88.52	96.16	96.34	94.20	99.55	99.66	99.55	95.70
RT 3	Best field pass rate	99.08	94.94	100.00	99.89	97.40	100.00	100.00	99.82	100.00	99.84
	Worst field pass rate	83.98	82.03	70.07	90.53	89.87	79.62	98.47	99.14	99.85	90.55
	Average field pass rate	91.10	90.08	88.85	95.30	94.75	94.05	99.37	99.53	98.71	95.73
RT 4	Best field pass rate	98.09	89.93	100.00	99.70	95.22	100.00	100.00	99.75	100.00	96.34
	Worst field pass rate	82.84	81.94	73.07	90.48	90.61	86.77	98.21	98.56	99.01	91.77
	Average field pass rate	90.48	86.23	86.19	95.53	93.35	94.20	99.46	99.42	99.60	94.12
RT 5	Best field pass rate	99.85	98.44	99.92	99.99	99.61	99.90	100.00	100.00	99.99	98.75
	Worst field pass rate	78.60	80.72	61.74	92.80	89.70	76.23	99.60	99.08	94.98	72.88
	Average field pass rate	91.69	92.44	86.84	96.72	96.57	93.26	99.92	99.70	98.63	90.02
1% diff											
Canine Phantom	Best field pass rate	94.88	81.40	98.70	96.88	88.60	98.60	98.70	97.70	98.15	83.23
	Worst field pass rate	51.75	57.54	62.63	65.16	67.17	69.78	85.40	88.47	79.70	65.71
	Average field pass rate	76.38	72.40	73.43	83.34	79.11	79.87	94.41	92.62	89.53	74.74
RT 1	Best field pass rate	80.31	82.34	97.50	90.31	87.64	96.92	98.84	95.35	97.78	80.07
	Worst field pass rate	62.06	61.59	40.02	69.21	69.55	52.20	88.36	85.09	73.19	66.91
	Average field pass rate	69.16	71.54	61.42	78.78	78.31	70.21	94.04	90.07	84.20	72.21
RT 2	Best field pass rate	87.12	69.25	100.00	94.42	81.18	99.99	98.74	97.15	99.85	88.93
	Worst field pass rate	46.86	47.33	39.69	57.47	58.56	50.55	83.73	83.39	76.85	54.79
	Average field pass rate	61.44	61.46	58.09	72.92	74.74	70.41	92.02	93.47	90.30	67.63
RT 3	Best field pass rate	80.54	71.19	99.66	93.84	80.64	99.48	99.42	95.10	99.54	82.02
	Worst field pass rate	42.27	50.79	33.31	52.84	61.49	45.39	82.70	84.21	70.81	57.65
	Average field pass rate	58.22	60.02	57.23	69.55	71.68	68.59	90.81	91.17	87.65	66.63
RT 4	Best field pass rate	78.39	58.87	99.94	89.45	71.69	99.99	98.38	91.64	99.98	70.50
	Worst field pass rate	44.11	43.54	35.35	55.77	56.40	51.06	82.41	84.00	81.56	55.03
	Average field pass rate	60.53	49.98	57.58	72.39	62.83	69.93	91.38	87.55	90.44	63.00
RT 5	Best field pass rate	94.24	77.36	99.13	98.94	88.08	98.99	99.25	98.36	98.99	81.04
	Worst field pass rate	40.86	52.34	25.43	57.52	58.92	37.18	91.83	81.24	61.40	36.84
	Average field pass rate	64.68	64.62	55.37	76.32	76.24	67.25	95.33	91.92	85.35	60.56

Table 3 Matrix listing recommended clinical parameter settings for detecting shifts using the 2D EPID dosimetry function in PerFRACTION

Desired shift detection level	1 mm	3 mm	5 mm	5° yaw
3% difference	Not advised	97%	96%	73%
1% difference	89%	63%	62%	37%

2D, 2-dimensional; EPID, electronic portal imager device.

Columns indicate the desired shift detection level; the rows list the % difference setting in PerFRACTION. Each cell indicates which pass rate tolerance setting would be required to flag at least 1 field for each of the 5 cadaver heads and the solid water phantom as failing.

are more likely to be detected, and only once they are detected can they be properly diagnosed and rooted out of the system."[14] Our data confirm the findings, specifically that traditionally used gamma metrics have insufficient sensitivity to detect inter- and intrafraction setup errors meeting or exceeding commonly used PTV margins as for example those specified in NRG/Radiation Therapy Oncology Group protocols. Furthermore, our data provide baseline information on how an alternative metric, percent difference, which together with stringent pass/fail criteria for cranial IMRT/SRS has high sensitivity to the stated clinical setup error detection goal. A direct impact on the safety of delivery is expected because standardized criteria will discourage setting the pass/fail criteria too

generously, possibly masking delivery errors from discovery. Our data intend to provide a starting point for cranial IMRT/SRS plans only; other sites and treatment techniques will require a separate investigation to create appropriate pass/fail criteria. Another less commonly used analysis method for IMRT QA analysis is the dose gradient analysis method developed by Moran et al.[15] At the time this study was performed, PerFRACTION was still in the beta-testing phase, and this analysis method was not available.

Our next step after the implementation of EPID dosimetry for cranial IMRT/SRS patients is to implement a more comprehensive quality control program for these patients through using statistical process control.[16] Statistical process control will provide the data to move from consensus-based pass/fail criteria agreed on by the medical physics community to criteria that better reflect the uncertainties of a delivery system.

Conclusion

PerFRACTION 2D mode successfully detected setup errors outside our systematic error tolerance for IMRT (3-mm shift) and SRS (1 mm) when an appropriate analysis metric and pass/fail criteria was implemented. By interpreting which beam angles passed or failed, the user was able to use PerFRACTION to infer which specific translational setup error was introduced. In addition, our PerFRACTION 2D EPID data confirm data from other 2D DQA methods that percent difference may be more sensitive in detecting plan failure than gamma analysis. Standardized minimum pass/fail criteria should be implemented to avoid too many false negatives causing clinical dose delivery errors to be missed.

References

1. Partridge M, Evans PM, Mosleh-Shirazi A, et al. Independent verification using portal imaging of intensity-modulated beam delivery by the dynamic MLC technique. *Med Phys.* 1998;25:1872-1879.
2. Pasma KL, Dirkx ML, Kroonwijk M, et al. Dosimetric verification of intensity modulated beams produced with dynamic multileaf collimation using an electronic portal imaging device. *Med Phys.* 1999;26:2373-2378.
3. Mans A, Wendling M, McDermott L, et al. Catching errors with in vivo EPID dosimetry. *Med Phys.* 2010;37:2638-2644.
4. Mijnheer BJ, González P, Olaciregui-Ruiz I, et al. Overview of 3-year experience with large-scale electronic portal imaging device–based 3-dimensional transit dosimetry. *Pract Radiat Oncol.* 2015;5:e679-e687.
5. Low DA, Harms WB, Mutic S, et al. A technique for the quantitative evaluation of dose distributions. *Med Phys.* 1998;25:656-661.
6. Bogdanich W. Radiation offers new cures, and ways to do harm. *New York Times*. January 23, 2010.
7. Ford EC, Terezakis S, Souranis A, et al. Quality control quantification (QCQ): A tool to measure the value of quality control checks in radiation oncology. *Int J Radiat Oncol Biol Phys.* 2012;84:e263-e269.
8. Bojechko C, Phillps M, Kalet A, et al. A quantification of the effectiveness of EPID dosimetry and software-based plan verification systems in detecting incidents in radiotherapy. *Med Phys.* 2015;42:5363-5369.
9. Nelms BE, Rasmussen KH, Tome WA. Evaluation of a fast method of EPID-based dosimetry for intensity-modulated radiation therapy. *J Appl Clin Med Phys.* 2010;11:3185.
10. Hansen KS, Théon AP, Dieterich S, et al. Validation of an indexed radiotherapy head positioning device for use in dogs and cats. *Vet Radiol Ultrasound.* 2015;56:448-455.
11. Bojechko C, Ford E. Quantifying the performance of in vivo portal dosimetry in detecting four types of treatment parameter variations. *Med Phys.* 2015;42:6912-6918.
12. Kruse JJ. On the insensitivity of single field planar dosimetry to IMRT inaccuracies. *Med Phys.* 2010;37:2516-2524.
13. Kry SF, Molineu A, Kerns JR, et al. Institutional patient-specific IMRT QA does not predict unacceptable plan delivery. *Int J Radiat Oncol Biol Phys.* 2014;90:1195-1201.
14. Nelms BE, Chan MF, Jarry G, et al. Evaluating IMRT and VMAT dose accuracy: practical examples of failure to detect systematic errors when applying a commonly used metric and action levels. *Med Phys.* 2013;40:111722.
15. Moran JM, Radawski J, Fraass BA. A dose gradient analysis tool for IMRT QA. *J Appl Clin Med Phys.* 2005;6:62-73.
16. Gerard K, Grandhaye J-P, Marchesi V, et al. A comprehensive analysis of the IMRT dose delivery process using statistical process control (SPC). *Med Phys.* 2009;36:1275-1285.